

# Acetylglutamine facilitates motor recovery after brachial plexus root avulsion in rats by promoting motoneuronal survival and axonal remyelination

**Lin Wu**

University of South China

**Shuangxi Chen**

University of South China

**Bing He**

University of South China

**Guijuan Zhou**

University of South China

**Yan Xu**

University of South China

**Guanghua Zhu**

University of South China

**Juan Xie**

University of South China

**Limin Deng**

University of South China

**Xuanwei Wen**

University of South China

**Sijing Li**

University of South China

**Zijian Xiao** (✉ [zijian6340@21cn.com](mailto:zijian6340@21cn.com))

University of South China

---

## Research Article

**Keywords:** Acetylglutamine (NAG), Brachial plexus root avulsion (BPRA), motoneuron (MN), inflammation, pyroptosis

**Posted Date:** February 9th, 2023

**DOI:** <https://doi.org/10.21203/rs.3.rs-2528484/v1>

**License:**  This work is licensed under a Creative Commons Attribution 4.0 International License.

[Read Full License](#)

---

**Version of Record:** A version of this preprint was published at Journal of Translational Medicine on August 23rd, 2023. See the published version at <https://doi.org/10.1186/s12967-023-04399-7>.

# Abstract

**Background:** Brachial plexus root avulsion (BPRA) is a disabling peripheral nerve injury that induces substantial death of motoneurons, degeneration of motor axons and de-innervation of biceps muscles, leading to loss of upper limb motor function. Acetylglutamine (N-acetyl-L-glutamine, NAG) has been proved to exert neuroprotective and anti-inflammatory effects in various disorders in the nervous system. Hence, the present study focused on the effect of NAG on motor recovery after BPRA in rats and the underlying mechanisms.

**Methods:** Adult male Sprague Dawley rats were subject to BPRA and reimplantation surgery and subsequently treated with NAG or saline. Behavioral tests were conducted to evaluate motor function recovery and mechanical pain threshold of the affected forelimb. The morphological appearance of the spinal cord, musculocutaneous nerve, and biceps brachii was assessed by histological staining. Quantitative real-time PCR was utilized to measure the mRNA levels of remyelination and regeneration indicators on myocutaneous nerves. The protein levels of inflammatory and pyroptotic indicators in the anterior horn of the spinal cord were measured using Western blot analysis.

**Results:** Our results indicated NAG could significantly accelerate recovery of motor function in the injured forelimbs, enhance motoneuronal survival in the anterior horn of the spinal cord, inhibit the expression of proinflammatory cytokines and pyroptosis pathway, facilitate axonal remyelination in the myocutaneous nerve and alleviate atrophy of biceps brachii. Additionally, NAG attenuated neuropathic pain following BPRA.

**Conclusion:** NAG promotes functional motor recovery by enhancing motoneuronal survival and axonal remyelination and inhibiting the pyroptosis pathway after BPRA in rats, laying the foundation for NAG to be a novel strategy for BPRA treatment.

## 1. Introduction

Over the years, the increase in the number of domestic motorcycles and the lack of safety awareness of drivers has been paralleled by an increase in traffic accidents, leading to a surge in the prevalence of brachial plexus root avulsion (BPRA)[1]. It has been established that BPRA induces the massive death of motoneurons, degeneration of motor axons and de-innervation of targeted biceps muscles, eventually resulting in loss of motor function in the upper extremity [2, 3]. The permanent disability of the upper extremities caused by BPRA affects patients significantly and represents a burden for families and society [4]. To facilitate motor function recovery after BPRA, different types of treatments such as surgical nerve reimplantation [5] can be carried out. However, axons of motor neurons grow too slowly to reinnervate target muscles, resulting in poor clinical prognosis after nerve reimplantation [6]. It has been shown that avulsion of ventral roots may result in extensive degeneration of motoneurons in the anterior horn of the spinal cord [7]. Koliatsos et al. demonstrated that ventral root avulsion causes 80% motor neuron retrograde death within the first 2 weeks after it occurs [8]. Promoting the survival of the injured

motor neurons is a prerequisite for functional motor recovery after BPRA [9]. Accordingly, the exploration of novel medical approaches is essential to accelerate the survival of motoneurons combined with reimplantation surgery during BPRA treatment.

Acetylglutamine (N-acetyl-L-glutamine, NAG), the derivative of glutamine and generated by the acetylation of glutamine [10], can produce two metabolites, including g-aminobutyric acid (GABA) and glutamic acid (Glu) [11]. GABA can promote acetylcholine activity and maintain normal brain function [12]. Moreover, Glu is an excitatory neurotransmitter tightly associated with the plasticity of neurons, playing a vital role in the growth of neurons and the generation of synapses [13]. Accumulated evidence has confirmed that NAG can exert a neuroprotective effect following cerebral ischemia-reperfusion injury via neuronal apoptosis and inflammation attenuation [12]. NAG has been reported to cross the blood-brain barrier (BBB) and exert multiple beneficial effects on neurological diseases [11]. Since they are easily accessible and affordable, NAG injections are extensively used to treat hepatic coma, hemiplegia, brain trauma, and sequelae of cerebral apoplexy.

Given the essential roles of NAG in the normal and diseased nervous system, we hypothesized that NAG might promote motor function recovery in rats following BPRA. Herein, we documented that NAG could inhibit inflammation and promote motoneuron survival, axon remyelination, and biceps brachii atrophy to accelerate the motor function recovery in rats following BPRA.

## 2. Materials And Methods

### 2.1 Animals

Adult male Sprague Dawley rats weighing 210–250 g were purchased from Changsha Tianqin Biotechnology Co., Ltd. All animals were housed in the Department of Laboratory Animal Science at the University of South China. The light cycle was maintained at 12h light and 12h dark, the room temperature kept at 18–22°C and relative humidity controlled between 50–60%. Rats had free access to drinking water and food. All experimental procedures were approved by The Laboratory Animal Ethics Committee of The First Affiliated Hospital of the University of South China.

### 2.2 Brachial plexus avulsion-re-implantation surgery

As shown in Fig. 1A, the surgical procedures on rats were performed based on previously described methods [9, 14]. Rats were anesthetized by intraperitoneal injection of 10% chloral hydrate at a dose of 5 µL/g. After removing the back hair, the rats were fixed on a foam table in the prone position. After cutting the skin, muscle and fascia, the C5, C6, and C7 spinal cord segments were accurately identified under a dissecting microscope. The right lamina segments of the rat were removed from the fourth cervical (C4) to the sixth cervical (C6), and the C5-C7 spinal cord segment was exposed under a surgical microscope. After opening the dura mater, the right-sided C5-C7 dorsal and ventral roots were avulsed by traction with fine glass hook. Then, the C6 ventral root was immediately reimplanted to the exact detached point after avulsion. The proximal residual rootlets and the distal parts of C5 and C7 were cut and removed to

prevent any regeneration. Care was taken to avoid any injury to the spinal cord. Finally, muscles and skin were sutured, and the rats were put back into their cages.

## **2.3 Grouping and treatments**

After the rat model of BPRA was established, the rats were randomly divided into 3 groups: Sham group, NS group and NAG group, with 6 rats in each group. Rats in the NAG group were given a subcutaneous injection of acetylglutamine solution (300 mg/kg.d) near the injury site, while rats in the Sham and NS groups were subcutaneously injected with an equal volume of normal saline for 7 consecutive days.

## **2.4 Behavioral tests**

### **2.4.1 Terzis grooming test**

The Terzis grooming test was performed to evaluate the motor function of the affected forelimbs as previously described in the literature [3, 9, 15]. Water was sprayed on the head of the rat from multiple directions to elicit a grooming reaction, and the rat was placed in a glass cylinder. A 5-minute video was recorded to elicit grooming movements of the forepawstowards the head when water was sprayed on the head of the rat. The scoring criteria are described as follows: 0, the affected limb does not move at all; 1, the affected limb has the elbow flexion reflex but cannot touch the nose; 2, the affected limb has the elbow flexion reflex and can touch the nose; 3, the affected limb has elbow flexion reflex and can touch below the eyes; 4 points, the affected limb has elbow flexion reflex and can touch the eyes; 5 points, the affected limb has the elbow flexion reflex and can touch the ear and the part behind the ear. The highest score was recorded within 5 minutes according to the above scoring criteria.

### **2.4.2 Cylinder Test**

A Cylinder Test was performed to evaluate the motor function of the affected forelimbs as described in the literature [16, 17]. The rat was placed in a glass cylinder (50 cm in diameter, 70 cm in height). The number of times the right forepaw touched the cylinder wall was recorded by video until the left forepaw reached 20 times.

### **2.4.3 Food-Pellet Taking Test**

The food-Pellet Taking Test was performed to evaluate the motor function of the affected forelimbs as previously described [16, 18]. After the rats fasted for 24 hours, they were videotaped as they ate uniform-sized cereals (spheres). Rats were then scored on the Irvine, Beatties and Bresnahan forelimb scale (IBB) scale for joint position, object support, finger movement, and grasping technique on a scale of 0–9.

### **2.4.4 Mechanical Withdrawal Threshold**

Mechanical pain threshold testing was performed to reflect changes in the animals' neuropathic pain behavior as documented in the literature[19, 20]. After the rats were kept quiet, the mechanosensitivity was tested with a series of Von Frey filaments (from thin to thick). The skin on the lateral plantar part of the foot was stimulated vertically with fibrils, and the fibrils were slightly bent for 5 s. When the rat

showed the paw withdrawal response, the same filament was selected for each interval of 5 minutes, and the paw withdrawal response occurred more than 3 times in 5 consecutive measurements, and the corresponding fiber filament grams were recorded. If no paw withdrawal response was observed within the 5 s test period, the adjacent fiber filaments were used to re-test until the paw withdrawal response occurs within 5 s.

## 2.5 Tissue Preparation

Rats were sacrificed after chloral hydrate anesthesia.

For qRT-PCR analysis, total RNA was extracted from myocutaneous nerve tissue with TRIzol reagent according to the manufacturer's protocol (Invitrogen), as described in the literature.

For Western blot analysis, spinal cord anterior horn tissue from C5-C7 segments was dissolved in 100 µl RIPA buffer containing 1% PMSF (0754, Amresco). After homogenization with an electric tissue homogenizer (Fluka), the supernatant was collected by centrifugation at 13,000 g for 20 min at 4°C.

For histological staining, rats were perfused transcardially with saline followed by 4% paraformaldehyde (PFA) until rigidity. Spinal cords, musculocutaneous nerves, and biceps were dissected and collected for further analysis. After fixation in 4% PFA for 24 hr at 4°C, tissues were transferred into a solution of PBS containing 15% and 30% sucrose for 24 hr at 4°C, respectively. The tissues were then cut into sections on a sliding microtome (LEICA CM1950, Leica).

## 2.6 Histochemical Staining

### 2.6.1 Nissl staining

Spinal cord sections were stained with Nissl's staining for 2–5 min, and 0.1% glacial acetic acid was used to process the sections until Nissl bodies were dark blue and the background was light blue or colorless. Images used for observation were digitalized by light microscopy (MBF Nikon Microscope). The number of motor neurons was counted using ImageJ 5.0 software.

### 2.6.2 Luxol fast blue (LFB) staining

Myelin stain A was heated in a 65°C oven for 30 min in advance. Musculocutaneous nerve sections were stained in Myelin A for 4 h at 65°C. Sections were processed in Myelin Stain B for 5 s and placed in Myelin Stain C for 10 s. Images used for observation were digitalized by light microscopy (MBF Nikon Microscope). The diameter of nerves was measured, and the number of nerve fibers was counted using ImageJ 5.0 software.

### 2.6.3 Hematoxylin and eosin (H&E) staining

Biceps brachii sections were first stained with hematoxylin for 3–5 min for nuclei staining. After soaking in hematoxylin solution for 2–5 s, the sections were stained with eosin staining solution for 5 min to ensure cytoplasmic staining. Finally, the tissue was dehydrated three times with absolute ethanol for 5

min each. Images used for observation were digitalized by light microscopy (MBF Nikon Microscope). The diameter of muscle fibers was measured, and the number of fibroblast nuclei was counted using ImageJ 5.0 software.

## 2.7 Quantitative real-time PCR (qRT-PCR)

Total RNA was extracted using TRNzol pure reagents (Tiangen Biotech, Beijing, China) from the sectioned C5-C7 spinal cord tissues in each group, and the isolated RNA was then electrophoresed on 1% agarose gel for purity examination. RNA concentration was measured using NanoDrop 2000 instrument (Thermo Scientific, Rockford, IL, USA). One microgram of total RNA was reverse-transcribed to first-strand cDNA using PrimeScript™ RT reagent Kit with gDNA Eraser (TaKaRa). The resultant cDNA was used as a template for the subsequent PCR amplification using SYBR GREEN Master Mix (Solarbio, Beijing, China), and the PCR reaction was performed on an ExicyclerTM 96 Real-Time PCR System (ABI7500, Applied Biosystems). The primer sequences for qRT-PCR used are shown in Table.1. A melting curve analysis was performed to confirm the single PCR product. The level of each gene was calculated according to the  $2^{-\Delta\Delta CT}$  method.

Table 1  
Primer Sequences for qRT-PCR

<b>Genes</b>		<b>Toward (5' to 3')</b>	<b>Sequences(bp)</b>
hmgcr	F	GTGGCCTCCATTGAGATCCG	258
hmgcr	R	ATGCACCGGGTTATCGTGAG	
prx	F	GAACTCTGGAGGTGTCTGGAG	88
prx	R	TTGAGGTCTTGCCTGCCTGAG	
mpz	F	AGATGCCATTCAATCTTCAC	151
mpz	R	GTGCCGTTGTCACTGTAGTCT	
pmp22	F	CCTACTGCCCTTGCTTTG	101
pmp22	R	TAGCCTCAGGCACAAACTCG	
egr2	F	TCAGTCCAACCCCTCTCAA	86
egr2	R	CATTGCTCCTCGCACAAACC	
L1CAM	F	CGAGTACAGGTCCCTGGAGA	163
L1CAM	R	TTGGCCGATGAAAGAGCCAT	
GAP-43	F	GATGCGGCCCTTCAGAGGAA	134
GAP-43	R	GGCACATCGGCTTGTAGGC	
pou3f1	F	TGGGCCTAGCGCACCCCTCAAT	154
pou3f1	R	ACCAAGCGGGCGTGGAAACCT	
ngfr	F	CATCTTGGCTGCTGTGGTCGT	197
ngfr	R	TCTGCGTATGGGTCTGCTGGT	
notch1	F	ACTATGGTTGTGCAAGGATG	134
notch1	R	CATAAGCAGAGGTAGTAGTTGTCA	
sox2	F	CTCCATGACCAGCTCGCAGAC	165
sox2	R	GCCCTGGAGTGGGAGGAAGAG	
GAPDH	F	CGTATCGGACGCCCTGGTT	83
GAPDH	R	AGGTCAATGAAGGGTCGTT	

## 2.8 Western Blot Analysis

20 µg of total protein were loaded onto sodium dodecyl sulfate-polyacrylamide gel electrophoresis (SDS-PAGE) of different concentrations for electrophoresis and transferred to a nitrocellulose filter membrane (NC, 0.45µm pore size, EMD Millipore Corporation, USA). Membranes were blocked with 5% skimmed milk in TBST (Tris-buffered saline, 0.1% Tween 20) for 1 h at RT and incubated with the primary antibodies overnight at 4°C. The primary antibodies used are shown in Table 2. Subsequently, the membranes were washed 5 times with TBST and incubated with goat anti-mouse IgG horseradish peroxidase (HRP)-conjugated secondary antibodies (1:10000, Tianderui Biotech., Beijing, China) for 40 min at RT. Immunoreactive proteins were detected using enhanced chemiluminescence (ECL) Western blotting detection kit (EMD Millipore Corporation, USA). The protein bands were scanned and quantified by Total Lab Quant V11.5 (Newcastle upon Tyne, UK).

Table 2 Primary antibody for Western Blot

Anti-nNOS antibody	ab76067	Abcam
Anti-p-Akt1 antibody	ab8805	Abcam
Anti-GAP-43 antibody	ab75810	Abcam
Anti-p-p65 antibody	ab31624	Abcam
Anti-TNF-α antibody	ab215188	Abcam
Anti-IL-6 antibody	ab233706	Abcam
Anti-IL-1β antibody	ab254360	Abcam
Anti-IL-18 antibody	ab243091	Abcam
Anti-c-Fos antibody	ab222699	Abcam
Anti-NGF antibody	ab52918	Abcam
Anti-CGRP antibody	ab272713	Abcam
Anti-GSDMD antibody	ab219800	Abcam
Anti-NLRP3 antibody	ab263899	Abcam
Anti-Caspase-1 antibody	ab207802	Abcam
GAPDH	YM3029	Immunoway

## 2.9 Statistical Analysis

All statistical analyses were performed using GraphPad Prism6 software. Data were expressed as mean ± SD and performed using Student's t-test. A *P*-value < 0.05 was statistically significant.

## 3. Results

### **3.1 NAG treatment increased body weight in rats following BPRA.**

To investigate the effect of NAG on the growth of rats subjected to BPRA, the body weights were measured every week after injury. As shown in Fig. 1C, 4 weeks to 8 weeks after surgery, a significant body weight loss was observed in the NS group compared to the sham group, while the body weight of all NAG-treated rats was significantly increased. Our findings suggested that NAG could induce an increase in body weight, confirming that NAG could promote the growth of rats.

### **3.2 NAG treatment accelerated recovery of motor function in the injured forelimbs of rats following BPRA.**

To evaluate recovery of motor function in the injured forelimbs of rats after BPRA, grooming tests and cylinder tests were performed weekly, and Food-Pellet Taking Test was performed at 8 weeks postoperatively.

Before surgery, all rats exhibited normal elbow flexion with a mean score of 5 before surgery. As shown in Fig. 2A-D, rats in the NS and NAG groups had a TGT score of 0 one week after BPRA injury, indicating a complete loss of motor function and proving the surgery's success. Recovery of motor function was observed two weeks after surgery. Moreover, the average TGT scores 2 to 8 weeks after surgery in the NAG-treated group were significantly improved compared with the NS group. At 8 weeks postoperatively, a score of 4 was observed in 80% and 20% of rats in the NAG-treated and NS groups, respectively.

Before surgery, all rats exhibited a similar ability to use both forelimbs. As shown in Fig. 2E-F, compared to the sham group, rats in the NS group exhibited decreased right forelimb use on the lesioned side (ipsilesional) after surgery. 2 to 8 weeks postoperatively, right forelimb use in the NAG-treated group was significantly higher than in the NS group.

To assess skilled forelimb function, we measured the ability to grasp and lift small pellets with the fingers and bring morsels to the mouth. To quantify measurements, the IBB score was used. As shown in Fig. 2G-H, before surgery, all the animals take food pellet with a mean score of 9. Compared to the sham group, the average IBB scores after surgery decreased in the NS group. In contrast, the average IBB scores were significantly increased in the NAG-treated group compared to the NS group.

These results indicated that NAG yielded a good recovery of motor function of the injured forelimbs in rats following BPRA.

### **3.3 NAG treatment enhanced motoneuronal survival in the anterior horn of the spinal cord in rats following BPRA.**

To investigate the effect of NAG on motoneuronal survival after ventral root avulsion/reimplantation, nissl staining was performed on spinal cord tissue. Moreover, we examined the expression levels of

neuronal survival-associated proteins, including growth-associated protein-43 (GAP-43), phosphorylated (p)-Akt, and neuronal nitric oxide synthase (nNOS) by Western Blot Analysis.

As shown in Fig. 3A-B, root avulsion resulted in extensive motoneuron loss in the ventral horns in the NS group compared to the Sham group. Moreover, treatment with NAG notably increased motoneuron survival in the NAG group compared to the NS group.

As shown in Fig. 3G-H, the expression of GAP-43 and p-Akt in saline-treated spinal cords were significantly downregulated compared to the sham group, while the levels of nNOS were upregulated. Conversely, treatment with NAG resulted in significant upregulation of GAP-43 and p-Akt levels compared with the saline-treated rats and could downregulate nNOS levels.

These results suggested that NAG exerts a protective effect against avulsion-induced apoptosis in motoneurons.

**3.4 NAG treatment inhibited the expression of proinflammatory cytokines and the pyroptosis pathway in rats following BPRA.**

To investigate the mechanism underlying the beneficial effect of NAG on the survival of injured motoneurons, the expression of several proinflammatory cytokines and pyroptosis pathway-related proteins in the anterior horn of the spinal cord were quantified by Western blot.

As shown in Fig. 4A-P after BPRA injury, the levels of the IL-1 $\beta$ , IL-18, IL-6, TNF- $\alpha$  and p-p65 in saline-treated rats were significantly higher than in the sham group, while IL-1 $\beta$ , IL-6, TNF- $\alpha$  and p-p65 protein expression was significantly downregulated in NAG-treated rats. Although the IL-18 levels were decreased after NAG treatment, the difference was not statistically significant. Moreover, NLRP3, GSDMD, and caspase-1 protein expression levels in the anterior horn of the spinal cord in the NS group were significantly higher than in the sham group. The expression of the NLRP3, GSDMD, and caspase-1 proteins was downregulated in the NAG-treatment group.

The above results suggest that the protective effect of NAG on motoneurons is tightly associated with the inhibition of inflammation and the pyroptosis pathway.

### **3.5 NAG treatment facilitated axonal remyelination in the myocutaneous nerve in rats following BPRA.**

To investigate the effects of NAG on the morphology of myocutaneous nerves in BPRA rats, myocutaneous nerve tissue was stained for LFB. We further explored whether the improved myocutaneous nerve morphology was related to axonal remyelination of motoneurons. Quantitative real-time polymerase chain reaction (qRT-qPCR) was carried out to assess changes in the expression of myelination-related genes.

As shown in Fig. 5A-B, a significant decline in the number of LFB-positive axons was observed in saline-treated rats compared to the sham group. However, the number of LFB-positive axons on the lesioned side in the NAG group was significantly higher than in the NS group. Moreover, we observed that the diameter of the musculocutaneous nerve in the NS group was significantly smaller than in the sham group. Besides, the diameter of the musculocutaneous nerve in the NAG-treated group was higher in the saline-treated group.

As shown in Fig. 5C-N, remyelination-associated genes (egr2, GAP-43, hmgcr, L1CAM, mpz, pmp22, and prx) were downregulated in response to injury compared to the sham group. However, they were upregulated in the NAG-treated group after injury. The opposite findings were documented for demyelination-associated genes (ngfr, notch1, pou3f1, and sox2).

These results suggested that NAG could alleviate the morphology of the abnormal musculocutaneous nerve fibers and promote musculocutaneous nerve remyelination in rats following BPRA.

### **3.6 NAG treatment alleviated biceps brachii atrophy in rats following BPRA.**

To evaluate the degree of muscle atrophy in the groups after surgery, the biceps brachii muscles of both right (injury) and left (intact) forelimbs were weighted, and the ratio of right/left biceps brachii weight was calculated. Then, the histopathological changes in the biceps tissue were evaluated by hematoxylin and eosin (H&E) staining.

As shown in Fig. 6A-C, compared to the sham group, a significant decline in the weight of biceps brachii muscles on the lesioned side was observed in the NS group. However, the weight of biceps brachii muscles on the lesioned side was significantly increased in the NAG-treated group compared to the NS group. Similar patterns were observed for the biceps brachii muscle volume.

As shown in Fig. 6D-F, saline-treated muscle fibers displayed significantly smaller diameters and higher amounts of fibroblasts compared to the sham group, showing clear signs of muscular atrophy. Conversely, NAG-treated muscles fibers were bigger with clear myocyte nuclei and no apparent fibrosis, morphologically similar to normal fibers.

Overall, our results suggested that NAG could ameliorate muscle atrophy in the rat model of BPRA.

### **3.7 NAG treatment attenuated neuropathic pain in rats following BPRA.**

The mechanical withdrawal threshold (MWT) was determined weekly based on the withdrawal responses of the rat's right forepaw to mechanical stimulation delivered using von-Frey filaments. Moreover, we utilized Western blot to quantify three neuropathic pain-related proteins, including Calcitonin gene-related peptide (CGRP), nerve growth factor (NGF), and c-FOS, in the spinal dorsal horn.

As shown in Fig. 7A, we used rats with a pre-operative mechanical pain threshold of 15 g to compare changes in the MWT after BPRA injury. Compared with the sham group, the MWT of the right forepaw of saline-treated rats was significantly decreased at 4–8 weeks postoperatively. Notably, in rats treated with NAG, the MWT of the right forepaw was significantly higher than the NS group.

As shown in Fig. 7B-G, the protein levels of CGRP, NGF and c-FOS were significantly increased in the NS group, while this tendency was remarkably reversed for CGRP and NGF after treatment with NAG, which also resulted in decreased protein levels of c-FOS.

Overall, these findings indicated that NAG could alleviate neuropathic pain in rats following BPRA.

## 4. Discussion

In previous studies, we revealed the effects of artemisinin, berberine and neuregulin-1 on motor function recovery after BPRA [9, 14, 15]. In the current study, we demonstrated that NAG treatment combined with nerve reimplantation contributed to better functional recovery after BPRA via increasing motoneuron survival, accelerating motor axonal remyelination and reducing muscle atrophy, which may be associated with the inhibition of inflammatory response and the pyroptosis pathway.

Nowadays, neurological functional assessment is commonly carried out to determine the degree of the injury and the effect of potential strategies for treatment [15]. Although exogenous neurotrophic factors, including glial cell-derived neurotrophic factor (GDNF) and brain-derived neurotrophic factor (BDNF), have been substantiated to reduce the loss of motoneuron after BPRA, their application at the clinical level to treat human cases of BPRA is largely limited by their short half-time and inability to cross the BBB [3]. In recent years, NAG has been used in various diseases, including brain trauma, hepatic coma, hemiplegia, and sequelae of cerebral apoplexy due to its remarkable anti-inflammatory and neuroprotective effects [21]. Consistently, in the present study, NAG-treated rats exhibited recovery of motor function after BPRA, with higher mean TGT and IBB scores and increased the use of affected forelimbs in NAG-treated groups compared to the NS group.

To maintain the motoneurons survival after injury for functional restoration is quite necessary. It has been established that growth-associated protein-43 (GAP-43), phosphorylated (p)-Akt and neuronal nitric oxide synthase (nNOS) are important proteins involved in neuron survival and axon growth. GAP-43 is a specific phosphoprotein on the vertebrate nerve cell membrane, widely used as a marker for neuronal development, synaptic plasticity, and regeneration [22]. Moreover, an increasing body of evidence suggests that suppressing nNOS can protect against the death of the neurons subject to peroxynitrite cytotoxicity [3, 14]. Besides, the critical role of phosphorylation of Akt for neuronal survival and growth in traumatic injuries is widely documented [23, 24]. The present study found that motoneuron survival was enhanced in the NAG-treated group exhibiting higher GAP-43 and p-Akt levels and lower nNOS expression.

Spinal root avulsion is characterized by the excessive activation of lesion-infiltrating microglia/macrophages and astrocytes[7, 25] that produce proinflammatory cytokines to inhibit neuronal

survival [26]. Pyroptosis is a well-recognized form of programmed cell death associated with proinflammatory activity. In this regard, when the body is subjected to noxious stimuli, intracellular and extracellular signaling pathways induce the formation of intracytoplasmic inflammasome through a caspase-1-dependent classical apoptotic pathway and/or caspase-4/5/11-dependent non-classical pyroptosis pathway. This phenomenon results in caspase-1 or caspase-4/5/11 activation to promote the secretion of proinflammatory cytokines such as interleukin-1 $\beta$  (IL-1 $\beta$ ) and interleukin-18 (IL-18) leading to cell pyroptosis [27–29]. There is ample evidence to suggest that pyroptosis occurs extensively in diseases of the central nervous system[30, 31]. Accordingly, targeting the regulation of cell pyroptosis may lead to the regulation of disease inflammation. Our findings implied that NAG could prevent motoneuron loss by downregulating the levels of proinflammatory cytokines, including TNF- $\alpha$ , IL-6, IL-1 $\beta$ , IL-18, p-p65. Overall, we found that NAG could prevent motoneuron loss by downregulating the levels of NLRP3, Caspase-1, and GSDMD after BPRA.

Importantly, the reimplanted ventral spinal root creates a relatively permissive microenvironment for axonal regrowth and elongation in BPRA rats. Nonetheless, reimplantation alone is not enough for successful reinnervation in humans and rodents [5]. Consistently, Han et al. reported that NAG could promote neurite outgrowth in the SH-SY5Y neuronal cell and axonal regeneration with thicker remyelinated axons in a rat model of sciatic nerve injury [32]. Indeed, efficient remyelination of the regenerated axons in the BPRA rats has been associated with early functional recovery [33]. Importantly, NAG treatment can accelerate the regeneration of axons that innervate target muscles. In our study, treatment with NAG significantly increased the diameter of the musculocutaneous nerve and the number of LFB-positive axons. This observation may be explained by the accelerated axonal extension or enhanced axonal branching induced by NAG. Moreover, we showed that the remyelination-associated genes (L1CAM, GAP-43, pmp22, mpz, hmgcr, egr2, and prx) were downregulated while demyelination-associated genes (ngrx, notch1, pou3f1, and sox2) were upregulated in the NAG-treated rats, indicating the ability of NAG to potentiate axonal remyelination.

It is widely acknowledged that motor neuron axons deliver neurotransmitters into the synaptic cleft and yield a trophic effect on their controlled muscle fibers. Interestingly, after denervation, morphological alterations, including fibrosis and shrunken sarcoplasm, are induced in muscle fibers [34]. During muscle reinnervation, muscle fibers are clustered but are not scattered as in the uninjured biceps. Due to the death of MNs and failure to target myocytes again, the muscle fibers are inclined to be reinnervated by nearest axon sprouts, causing fiber-type grouping [35]. In our study, we found that NAG could efficiently alleviate muscle atrophy in rats subjected to avulsion/reimplantation, with higher biceps muscle weight and volume, larger fiber size and decreased number of fibroblast nuclei.

Neurogenic pain is a common and refractory complication after BPRA injury [36]. In addition to the motor and sensory deficits, pain can be equally debilitating. BPRA pain has been characterized as a rapid (an effect that occurs immediately after the trauma) and intermittent shooting pain, which may be observed at sites distant from the lesion. The pain states are generated and maintained by the activation of microglia and astrocytes in the spinal cord, which usually lasts 3 months after BPA [37]. Previous reports

have demonstrated that various nociceptive stimuli could activate c-Fos (a pain biomarker) in the spinal cord. NGF and CGRP have been substantiated to play a critical role in the molecular mechanisms of inflammatory-mediated disorders and are closely associated with nerve pain. Consistently, we observed that NAG could significantly reduce the MWT and the protein levels of NGF and CGRP, suggesting that NAG could possess pain-alleviating effects.

To the best of our knowledge, this is the first study to provide compelling evidence that acetylglutamine promotes functional motor recovery via enhancing motoneuronal survival and axonal remyelination after brachial plexus root avulsion in rats. Moreover, acetylglutamine may inhibit pyroptosis and attenuate the inflammatory response in the anterior horn of the spinal cord, leading to improved motoneuron survival. Importantly, we demonstrated that acetylglutamine could reduce neuropathic pain following brachial plexus avulsion. Taken together, acetylglutamine has huge prospects for clinical application to treat brachial plexus avulsions.

## Declarations

### Ethics approval and consent to participate

All experimental procedures were approved by The Laboratory Animal Ethics Committee of The First Affiliated Hospital of the University of South China.

### Consent for publication

I, the undersigned, give my consent for the publication.

### Conflicts of Interest

The authors declare no competing financial interest.

### Funding

We thank the Scientific research project of Hunan Health Committee (grant nos. 20201911, 20200469, 20211411761), Hunan Provincial Natural Science Foundation of China (grant nos. 2020JJ5512, 2021JJ30625, 2021JJ70114), Clinical medical technology innovation guidance project in Hunan Province (grant no. 2020SK51822) for support.

### Acknowledgment

None.

### Availability of data and material

All data generated or analyzed during this study are included in this published article.

### Author Contribution

Conceptualization, Z.X.; Methodology, L.W., S.C. and S.H.F.; Investigation, M.C., K.S., C.P. S.V. and S.H.F.; Writing –Original Draft, M.C., K.S., C.P., andS.H.F.; Writing –Review & Editing, M.C, K.S., C.P., and S.H.F.; Funding Acquisition,S.H.F.; Supervision, M.C., K.S., and S.H.F. All authors read and approved the fnalmanuscript.

## References

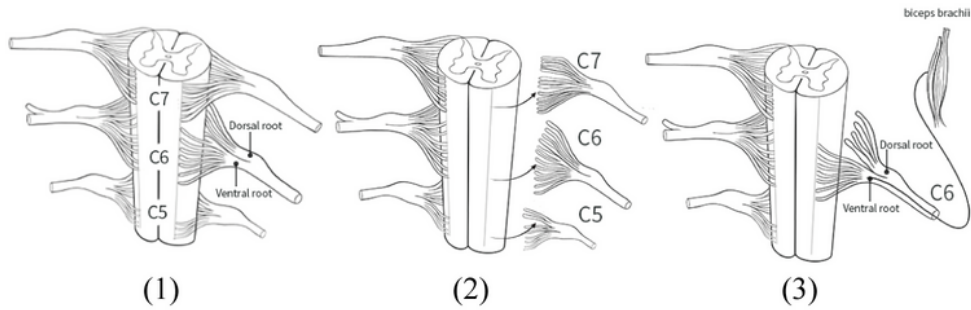
1. Kaiser R, Waldauf P, Haninec P. Types and severity of operated supraclavicular brachial plexus injuries caused by traffic accidents. *Acta Neurochir.* 2012;154(7):1293–7.
2. Umansky D, Midha R. Treatment of neuropathic pain after peripheral nerve and brachial plexus traumatic injury. *Neurol India.* 2019;67(Supplement):23–S24.
3. Zhang X, Liu XD, Xian YF, Zhang F, Huang PY, Tang Y, Yuan QJ, Lin ZX. Berberine enhances survival and axonal regeneration of motoneurons following spinal root avulsion and re-implantation in rats. *Free Radic Biol Med.* 2019;143:454–70.
4. Terzis JK, Vekris MD, Soucacos PN. Brachial plexus root avulsions. *World J Surg.* 2001;25(8):1049–61.
5. Gu HY, Chai H, Zhang JY, Yao ZB, Zhou LH, Wong WM, Bruce IC, Wu WT. Survival, regeneration and functional recovery of motoneurons after delayed reimplantation of avulsed spinal root in adult rat. *Exp Neurol.* 2005;192(1):89–99.
6. Araújo MR, Kyrylenko S, Spejo AB, Castro MV, Ferreira Junior RS, Barra viera B, Oliveira ALR. Transgenic human embryonic stem cells overexpressing FGF2 stimulate neuroprotection following spinal cord ventral root avulsion. *Exp Neurol.* 2017;294:45–57.
7. Barbizan R, Oliveira AL. Impact of acute inflammation on spinal motoneuron synaptic plasticity following ventral root avulsion. *J Neuroinflamm.* 2010;7:29.
8. Koliatsos VE, Price WL, Pardo CA, Price DL. Ventral root avulsion: an experimental model of death of adult motor neurons. *J Comp Neurol.* 1994;342(1):35–44.
9. Chen S, Wu L, He B, Zhou G, Xu Y, Zhu G, Xie J, Yao L, Huang J, Wu H, et al. Artemisinin Facilitates Motor Function Recovery by Enhancing Motoneuronal Survival and Axonal Remyelination in Rats Following Brachial Plexus Root Avulsion. *ACS Chem Neurosci.* 2021;12(17):3148–56.
10. Li X, Wang T, Zhang D, Li H, Shen H, Ding X, Chen G. Andrographolide ameliorates intracerebral hemorrhage induced secondary brain injury by inhibiting neuroinflammation induction. *Neuropharmacology.* 2018;141:305–15.
11. Ai J, Wan H, Shu M, Zhou H, Zhao T, Fu W, He Y. Guhong injection protects against focal cerebral ischemia-reperfusion injury via anti-inflammatory effects in rats. *Arch Pharm Res.* 2017;40(5):610–22.
12. Xu S, Li C, Zhou H, Yu L, Deng L, Zhu J, Wan H, He Y. A Study on Acetylglutamine Pharmacokinetics in Rat Blood and Brain Based on Liquid Chromatography-Tandem Mass Spectrometry and Microdialysis Technique. *Front Pharmacol.* 2020;11:508.

13. Granger AJ, Mulder N, Saunders A, Sabatini BL. Cotransmission of acetylcholine and GABA. *Neuropharmacology*. 2016;100:40–6.
14. Chen S, He B, Zhou G, Xu Y, Wu L, Xie Y, Li Y, Huang J, Wu H, Xiao Z. Berberine enhances L1 expression and axonal remyelination in rats after brachial plexus root avulsion. *Brain and behavior*. 2020;10(10):e01792.
15. Chen S, Hou Y, Zhao Z, Luo Y, Lv S, Wang Q, Li J, He L, Zhou L, Wu W. Neuregulin-1 Accelerates Functional Motor Recovery by Improving Motoneuron Survival After Brachial Plexus Root Avulsion in Mice. *Neuroscience*. 2019;404:510–8.
16. Han Q, Cao C, Ding Y, So KF, Wu W, Qu Y, Zhou L. Plasticity of motor network and function in the absence of corticospinal projection. *Exp Neurol*. 2015;267:194–208.
17. Huotarinen A, Leino S, Tuominen RK, Laakso A. Rat subthalamic stimulation: Evaluating stimulation-induced dyskinesias, choosing stimulation currents and evaluating the anti-akinetic effect in the cylinder test. *MethodsX*. 2019;6:2384–95.
18. Chang Q, Hanania T, Mash DC, Maillet EL. Noribogaine reduces nicotine self-administration in rats. *J Psychopharmacol (Oxford England)*. 2015;29(6):704–11.
19. Xie W, Kang Z, Jiang C, Liu N. Administration of Curcumin Alleviates Neuropathic Pain in a Rat Model of Brachial Plexus Avulsion. *Pharmacology*. 2019;103(5–6):324–32.
20. Yao M, Sun H, Yuan Q, Li N, Li H, Tang Y, Leung GK, Wu W. Targeting proteoglycan receptor PTP $\sigma$  restores sensory function after spinal cord dorsal root injury by activation of Erks/CREB signaling pathway. *Neuropharmacology*. 2019;144:208–18.
21. Zhang R, Yang N, Ji C, Zheng J, Liang Z, Hou CY, Liu YY, Zuo PP. Neuroprotective effects of Aceglutamide on motor function in a rat model of cerebral ischemia and reperfusion. *Restor Neurol Neurosci*. 2015;33(5):741–59.
22. Yu T, Zhao C, Hou S, Zhou W, Wang B, Chen Y. Exosomes secreted from miRNA-29b-modified mesenchymal stem cells repaired spinal cord injury in rats. *Brazilian J Med Biol research = Revista brasileira de pesquisas medicas e biologicas*. 2019;52(12):e8735.
23. Walker CL, Wu X, Liu NK, Xu XM. Bisperoxovanadium Mediates Neuronal Protection through Inhibition of PTEN and Activation of PI3K/AKT-mTOR Signaling after Traumatic Spinal Injuries. *J Neurotrauma*. 2019;36(18):2676–87.
24. Hou Y, Wang K, Wan W, Cheng Y, Pu X, Ye X. Resveratrol provides neuroprotection by regulating the JAK2/STAT3/PI3K/AKT/mTOR pathway after stroke in rats. *Genes & diseases*. 2018;5(3):245–55.
25. Yuan Q, Xie Y, So KF, Wu W. Inflammatory response associated with axonal injury to spinal motoneurons in newborn rats. *Dev Neurosci*. 2003;25(1):72–8.
26. Ohlsson M, Hoang TX, Wu J, Havton LA. Glial reactions in a rodent cauda equina injury and repair model. *Exp Brain Res*. 2006;170(1):52–60.
27. Hou AL, Xu WD. A model of neuropathic pain in brachial plexus avulsion injury and associated spinal glial cell activation. *J pain Res*. 2018;11:3171–9.

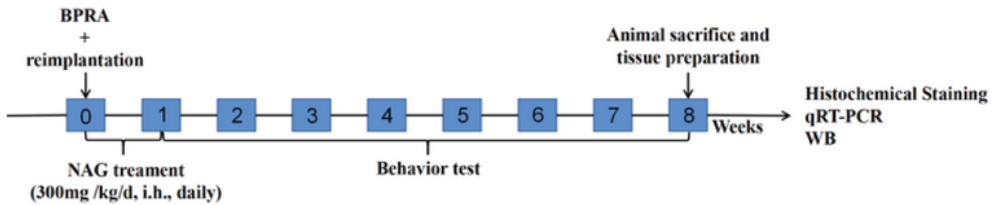
28. Hou AL, Zheng MX, Hua XY, Huo BB, Shen J, Xu JG. Electroacupuncture-Related Metabolic Brain Connectivity in Neuropathic Pain due to Brachial Plexus Avulsion Injury in Rats. *Front Neural Circuits*. 2020;14:35.
29. Huang H, Liu J, Hao H, Chen D, Zhizhong L, Li M, Song H, Xiang R, Jiang C, Fu X, et al. Preferred M2 Polarization by ASC-Based Hydrogel Accelerated Angiogenesis and Myogenesis in Volumetric Muscle Loss Rats. *Stem cells international*. 2017;2017:2896874.
30. Huang H, Liu J, Hao H, Tong C, Ti D, Liu H, Song H, Jiang C, Fu X, Han W. **G-CSF Administration after the Intraosseous Infusion of Hypertonic Hydroxyethyl Starches Accelerating Wound Healing Combined with Hemorrhagic Shock.** *BioMed research international* 2016, 2016:5317630.
31. Huo BB, Zheng MX, Hua XY, Shen J, Wu JJ, Xu JG. Brain Metabolism in Rats with Neuropathic Pain Induced by Brachial Plexus Avulsion Injury and Treated via Electroacupuncture. *J pain Res*. 2020;13:585–95.
32. Han AM, Heo H, Kwon YK. Berberine promotes axonal regeneration in injured nerves of the peripheral nervous system. *J Med Food*. 2012;15(4):413–7.
33. Fang XY, Zhang WM, Zhang CF, Wong WM, Li W, Wu W, Lin JH. Lithium accelerates functional motor recovery by improving remyelination of regenerating axons following ventral root avulsion and reimplantation. *Neuroscience*. 2016;329:213–25.
34. Connor EA, McMahan UJ. Cell accumulation in the junctional region of denervated muscle. *J Cell Biol*. 1987;104(1):109–20.
35. Kugelberg E, Edström L, Abbruzzese M. Mapping of motor units in experimentally reinnervated rat muscle. Interpretation of histochemical and atrophic fibre patterns in neurogenic lesions. *J Neurol Neurosurg Psychiatry*. 1970;33(3):319–29.
36. Xian H, Xie R, Luo C, Cong R. **Comparison of Different In Vivo Animal Models of Brachial Plexus Avulsion and Its Application in Pain Study.** *Neural plasticity* 2020, 2020:8875915.
37. Kachramanoglou C, Carlstedt T, Koltzenburg M, Choi D. Long-Term Outcome of Brachial Plexus Reimplantation After Complete Brachial Plexus Avulsion Injury. *World Neurosurg*. 2017;103:28–36.

## Figures

A



B



C

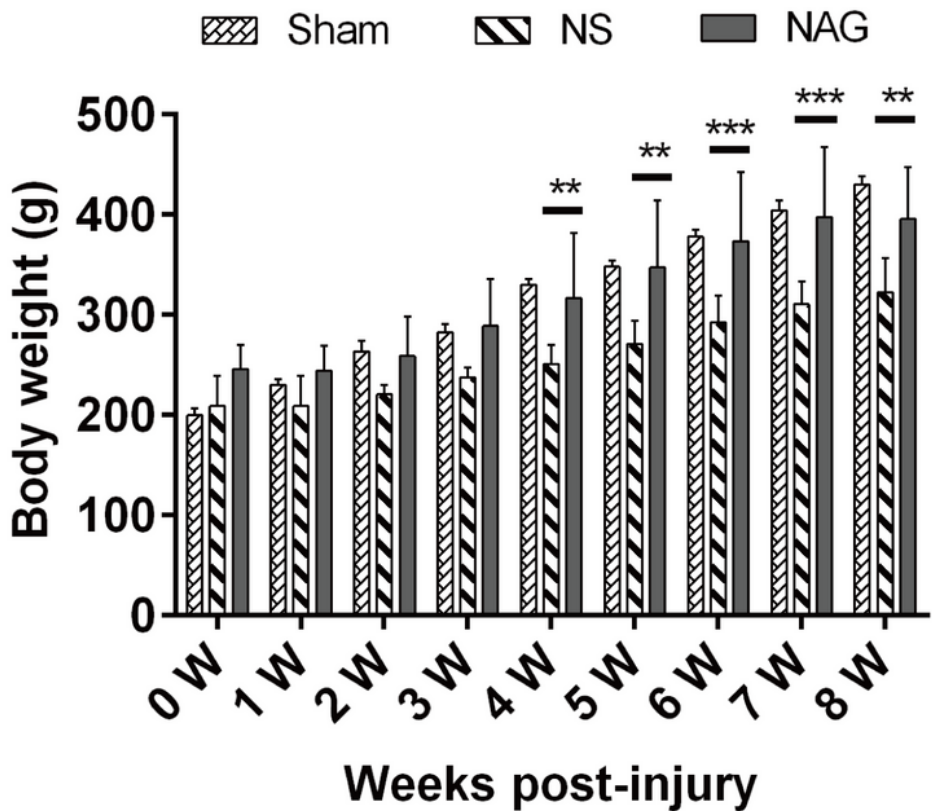
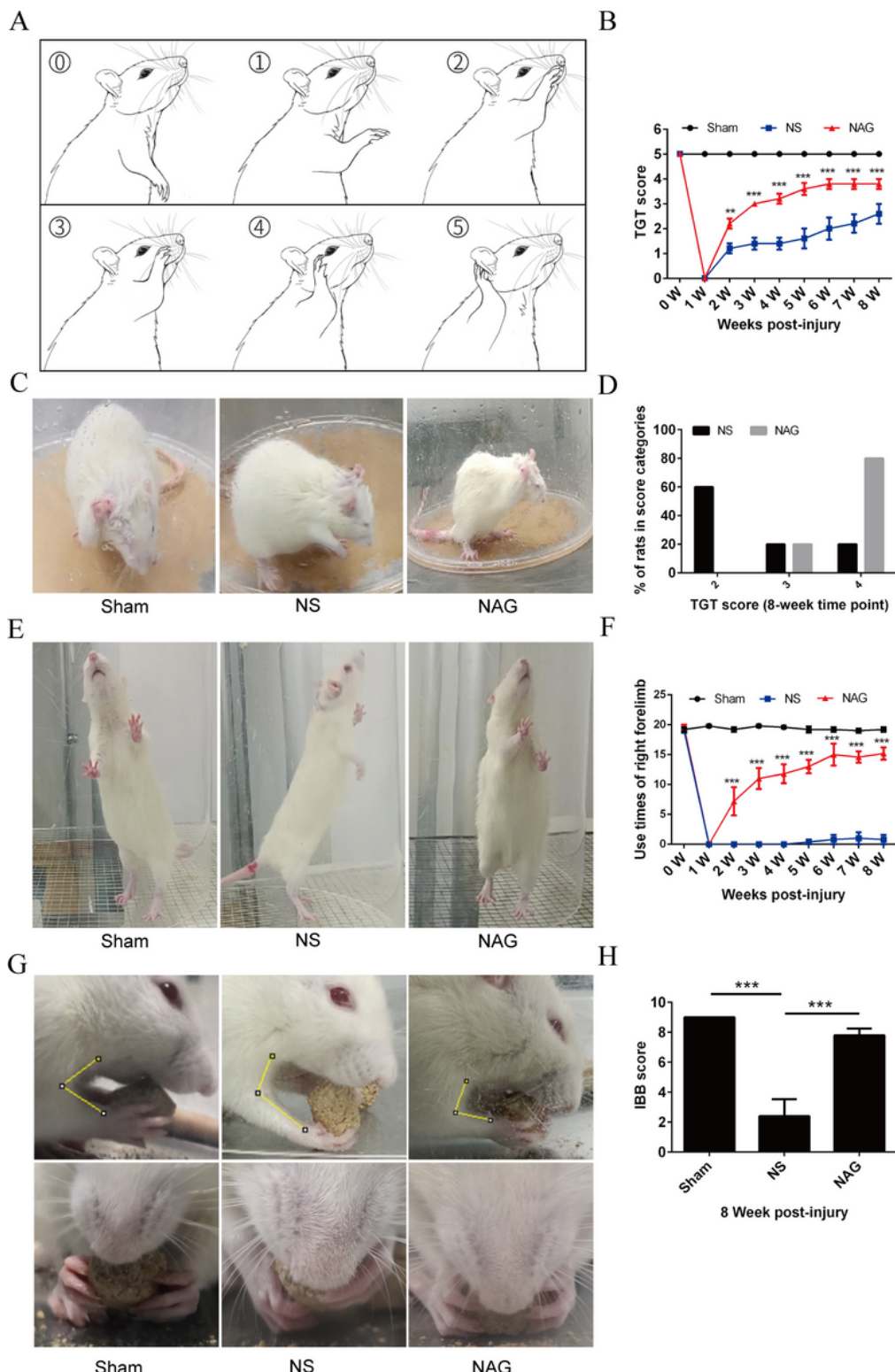


Figure 1

### Brachial plexus root avulsion and reimplantation model, experimental design and body weights of rats.

(A) Schematic drawing of the surgical procedures. (1) Anatomical structure of normal C5–C7 spinal cord segments; (2) the right C5-7 ventral and dorsal roots were avulsed; (3) the C6 ventral root was reimplanted to the surface of the corresponding spinal cord segment. (B) Schematic drawing of the workflow of the

experimental design. (C) The average body weights in all subgroups at each time point were shown. Data shown are mean  $\pm$  SD in each group; \*\*\* $P < 0.001$ , \*\* $P < 0.01$ , \* $P < 0.05$ .



**Figure 2**

**Effects of NAG treatment on motor functional recovery of the injured forelimbs.** (A) Schematic drawing of the Terzis grooming test (TGT) and rating criterion. (B) Photographs of TGT in each subgroup of rats. (C)

Average TGT scores in each subgroup of rats at each time-point. (D) The proportion of rats in each TGT score category in the NS and NAG group at 8 weeks postoperatively. (E) Photographs of the Cylinder Test in each subgroup of rats. (F) Averaged use times of right forelimb in each subgroup of rats at each time-point. (G) Photographs of Food-Pellet Taking Test in each subgroup of rats. (H) Averaged IBB scores in each subgroup of rats at 8 weeks postoperatively. Data shown are mean  $\pm$  SD in each group; \*\*\* $P < 0.001$ , \*\* $P < 0.01$ , \* $P < 0.05$ .

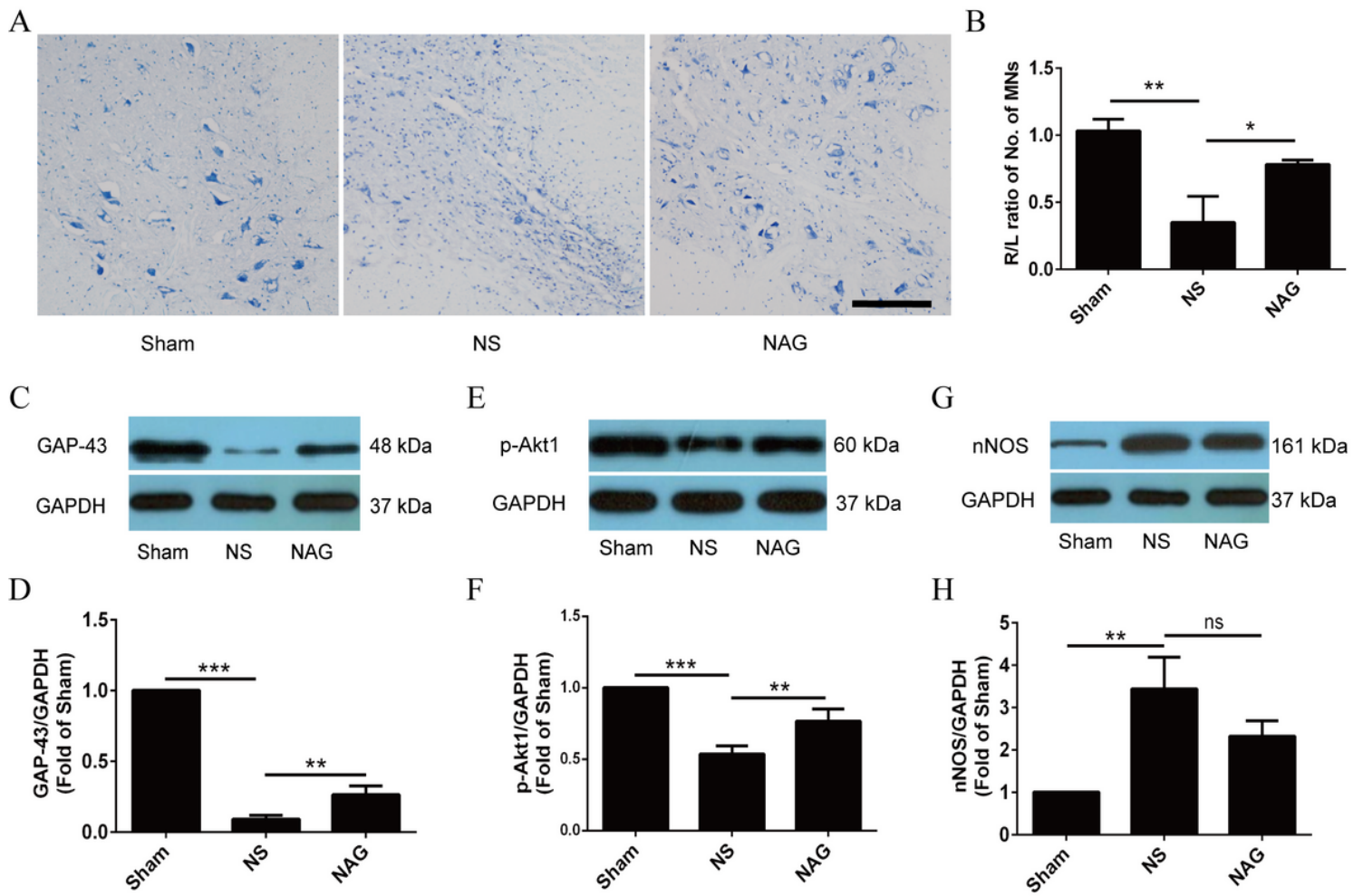


**Figure 3**

**Effects of NAG treatment on histological alteration and motoneuronal survival of spinal cord.** (A) Histological images of spinal cord sections with Nissl staining from all groups. Scale bar represents 20 $\mu$ m. (B) The survival rate of motoneurons was estimated as the percentage of the left (intact)/right (injury) motoneurons located in the ventral horn. The expression levels of GAP-43(C, D), p-Akt1(E, F) and nNOS(G, H) in the ventral horn of the spinal cord were determined using WesternBlot. Data shown are mean  $\pm$  SD in each group; \*\*\* $P < 0.001$ , \*\* $P < 0.01$ , \* $P < 0.05$ .

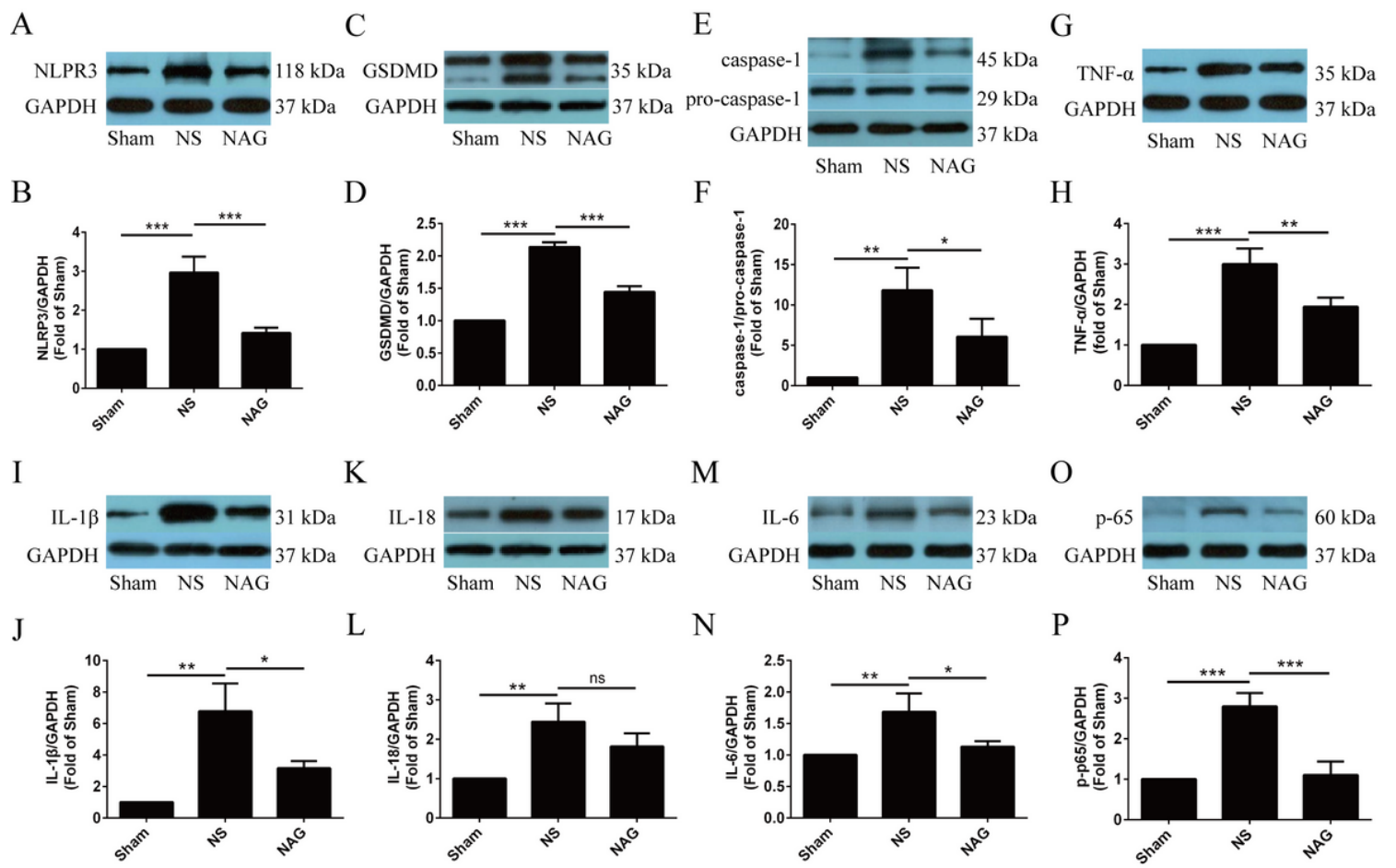


**Figure 4**

**Effects of NAG treatment on the expressions of IL-1 $\beta$ , IL-18, IL-6, TNF- $\alpha$ , p-p65, NLRP3, GSDMD, pro-caspase-1 and caspase-1 in the ventral horn.** The expression levels of NLRP3 (A, B), GSDMD (C, D), caspase-1/pro-caspase-1 (E, F), TNF- $\alpha$  (G, H), IL-1 $\beta$  (I, J), IL-18 (K, L), IL-6 (M, N) and p-p65 (O, P) in the ventral horn of spinal cord were determined using WesternBlot. Data shown are mean  $\pm$  SD in each group; \*\*\* $P$ < 0.001, \*\* $P$ < 0.01, \* $P$ < 0.05.

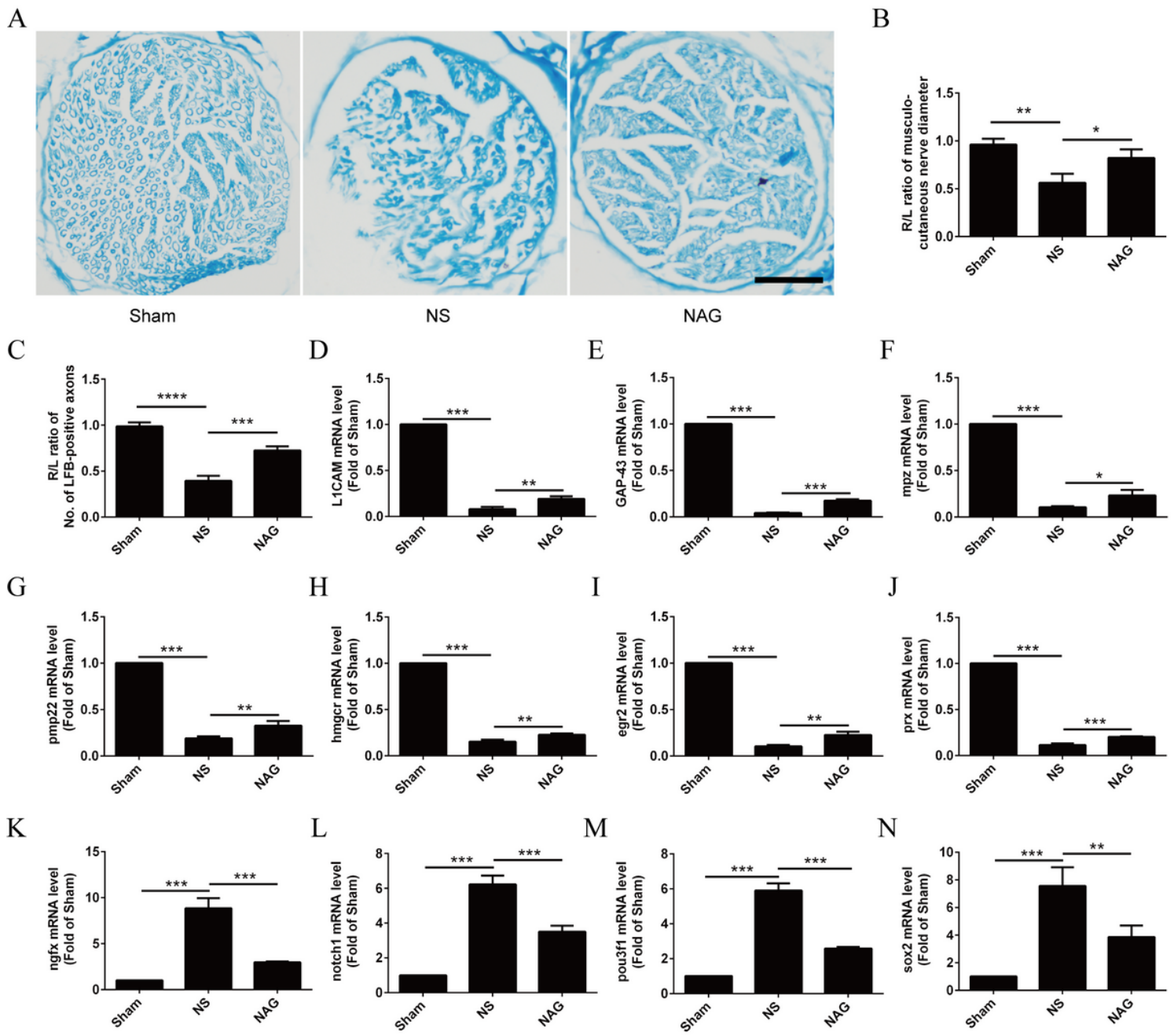


**Figure 5**

**Effects of NAG treatment on histological alterations and the remyelination of musculocutaneous nerves.**

(A) Histological images of musculocutaneous nerve sections with LFB staining from all groups. Scale bar represents 20 $\mu$ m. (B) Average ratio of the diameter of musculocutaneous nerves of the right (injury) to the left (intact) side at 8 weeks postoperatively. (C) Average ratio of the number of LFB-positive axons of the right (injury) to the left (intact) side at 8 weeks postoperatively. (D-J) mRNA levels of myelination-associated genes (egr2, GAP-43, hmgcr, L1CAM, mpz, pmp22, and prx) were determined using qRT-PCR. (K-N) mRNA levels of demyelination-associated genes (ngfr, notch1, pou3f1, and sox2) were determined using qRT-PCR. Data shown are mean  $\pm$  SD in each group; \*\*\*P < 0.001, \*\*P < 0.01, \*P < 0.05.

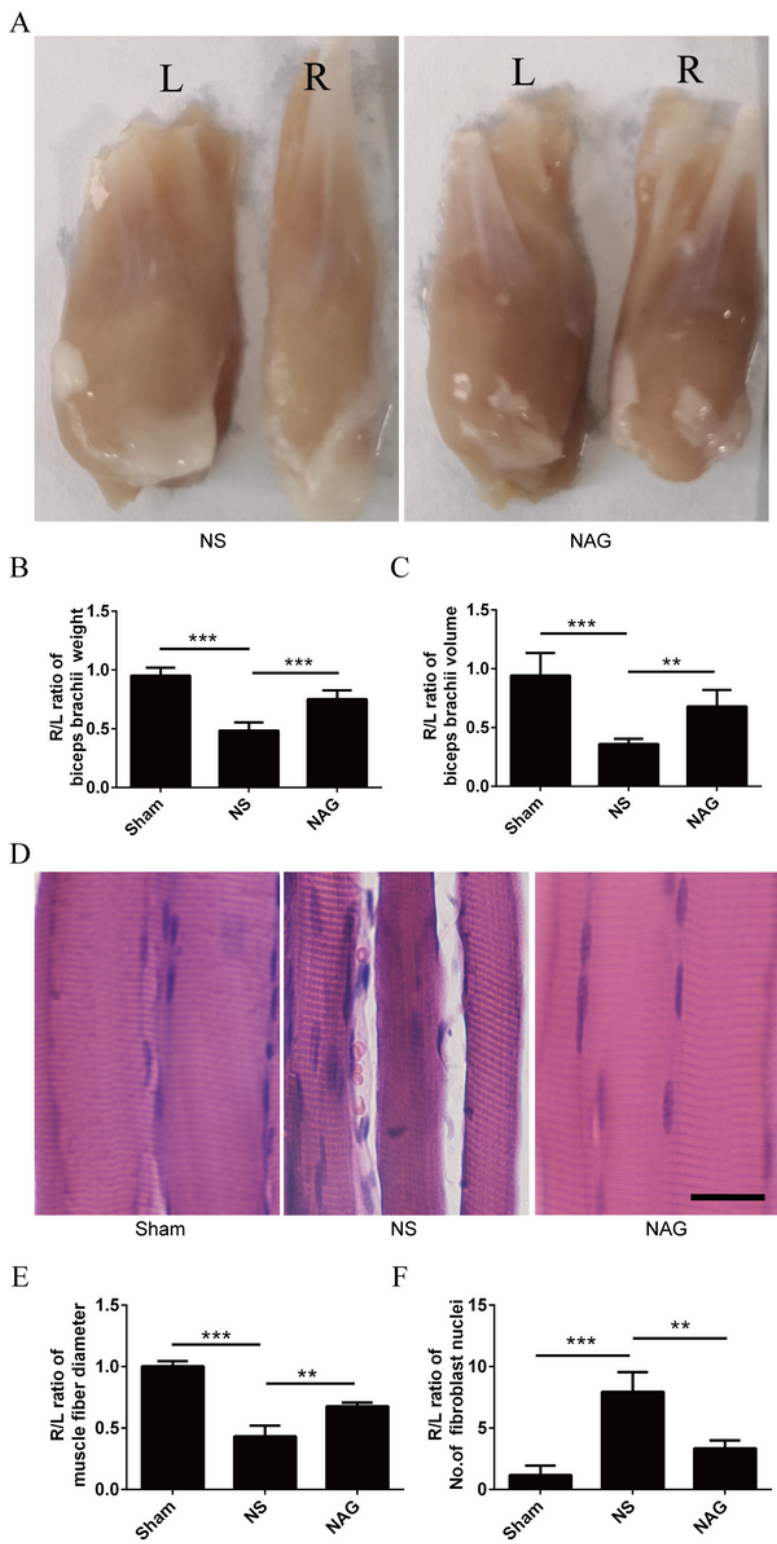


**Figure 6**

**Effects of NAG treatment on the weight and histological alteration of biceps.** (A) Representative photographs of biceps muscles from both ipsilateral and contralateral regions of the avulsed rats. Scale bar represents 2 mm. (B) Average ratio of biceps muscles wet weight of the right (injury) to the left (intact) side at 8 weeks postoperatively. (C) Average ratio of biceps muscle volume of the right (injury) to the left (intact) side at 8 weeks postoperatively. (D) Histological images of longitudinal bicep muscle

sections with H&E staining from all groups. Scale bar represents 100 $\mu$ m. (E) Average ratio of the muscle fiber diameter of the right (injury) to the left (intact) side. (F) The extent of fibrosis was calculated as the ratio of the number of fibroblast nuclei in the right (injury) to the left (intact) side. Data shown are mean  $\pm$  SD in each group; \*\*\*P < 0.001, \*\*P < 0.01, \*P < 0.05.

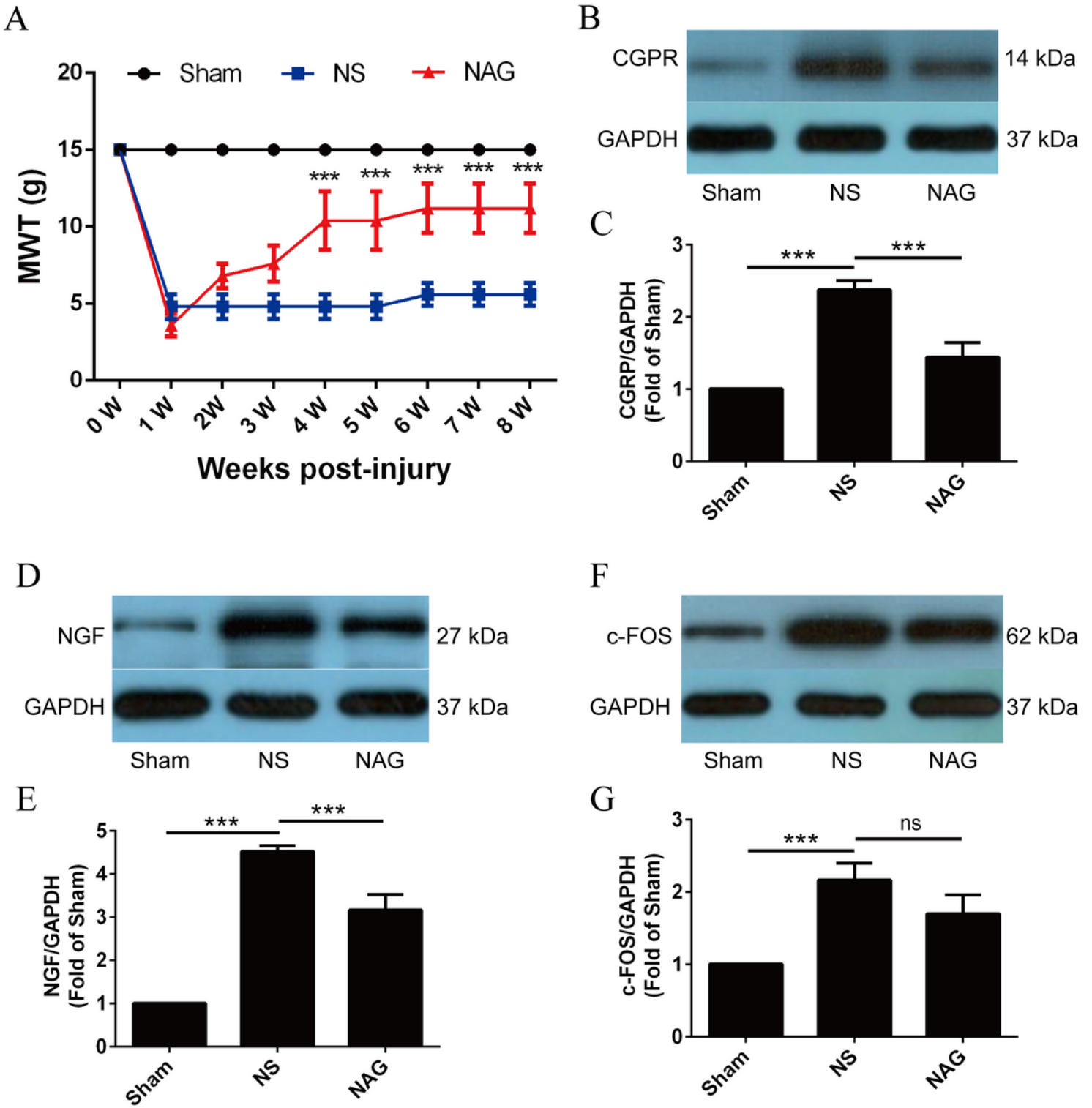


Figure 7

**Effects of NAG treatment on changes of MWT and the expressions of CRGP, NGF and c-FOS in the dorsal horn. (A)** Average MWT in each subgroup of rats at each time point. The expression levels of CRGP (**B, C**), NGF (**D, E**) and c-FOS (**F, G**) in the dorsal horn of the spinal cord were determined using WesternBlot. Data shown are mean  $\pm$  SD in each group; \*\*\* $P < 0.001$ , \*\* $P < 0.01$ , \* $P < 0.05$ .